

Intra-Cluster Mixup: An Effective Data Augmentation Technique for Complementary-Label Learning

Tan-Ha Mai

*Department of Computer Science and Information Engineering
National Taiwan University*

d10922024@csie.ntu.edu.tw

Hsuan-Tien Lin*

*Department of Computer Science and Information Engineering
National Taiwan University*

htlin@csie.ntu.edu.tw

Abstract

In this paper, we investigate the challenges of *complementary-label learning (CLL)*, a specialized form of *weakly-supervised learning (WSL)* where models are trained with labels indicating classes to which instances do not belong, rather than standard ordinary labels. This alternative supervision is appealing because collecting complementary labels is generally cheaper and less labor-intensive. Although most existing research in CLL emphasizes the development of novel loss functions, the potential of data augmentation in this domain remains largely underexplored. In this work, we uncover that the widely-used Mixup data augmentation technique is ineffective when directly applied to CLL. Through in-depth analysis, we identify that the complementary-label noise generated by Mixup negatively impacts the performance of CLL models. We then propose an improved technique called *Intra-Cluster Mixup (ICM)*, which only synthesizes augmented data from nearby examples, to mitigate the noise effect. ICM carries the benefits of encouraging complementary label sharing of nearby examples, and leads to substantial performance improvements across synthetic and real-world labeled datasets. In particular, our wide spectrum of experimental results on both balanced and imbalanced CLL settings justifies the potential of ICM in aligning with state-of-the-art CLL algorithms, achieving significant accuracy increases of 30% and 10% on MNIST and CIFAR datasets, respectively.

1 Introduction

Obtaining high-quality labels is often expensive, time-consuming, and sometimes impossible in real-world applications. To address this challenge, *weakly-supervised learning (WSL)* has been extensively studied in recent years. WSL aims to train a proper classifier with inaccurate, incomplete, or inexact supervision (Zhou, 2017). Contemporary WSL studies have significantly expanded our understanding of machine learning capabilities, encompassing areas such as learning from complementary labels (Ishida et al., 2017), learning from multiple complementary labels (Feng et al., 2020), learning from partial labels (Jin & Ghahramani, 2002), or a mixture of ordinary and complementary labels (Ishida et al., 2017).

This paper focuses on *complementary-label learning (CLL)* (Ishida et al., 2017), a WSL problem where a complementary label designates a class to which a specific instance *does not belong*. The CLL problem assumes that the learner only has access to complementary labels during training while still expecting the learner to predict the ordinary labels correctly during testing. Complementary labels serve as a viable alternative when it is difficult or costly to acquire ordinary labels (Ishida et al., 2017). For instance, collecting ordinary labels on numerous classes not only demands annotators with excellent knowledge for selecting the correct labels but also requires more time for accurate labeling. CLL models can extend the horizon of

*Corresponding author.

machine learning and make multi-class classification potentially more realistic when ordinary labels cannot be easily obtained (Ishida et al., 2017).

Existing CLL studies have primarily focused on designing loss functions that are converted from well-known ordinary classification losses (Ishida et al., 2017; Chou et al., 2020b; Ishida et al., 2018), often under the assumption that complementary labels are uniformly generated (Cao et al., 2022; Feng et al., 2020). Those loss-designing studies tackle the CLL problem *algorithmically* and enrich our understanding on possible CLL models. Despite this focus, the potential of data augmentation in CLL remains largely unexplored. This notable gap in the literature motivates our study on developing and assessing data augmentation techniques to improve the efficacy of CLL models.

Data augmentation techniques are known to be powerful “*add-ons*” to machine learning models for enhancing their performance by improving generalization, robustness to noise, and invariance to transformations (Mikołajczyk & Grochowski, 2018; Rebuffi et al., 2021). Across a range of classification scenarios (Chou et al., 2020a), successful data augmentation techniques exhibit seamless integration with algorithmic approaches to boost their performance. Some data augmentation techniques create pseudo examples that are variations of the original examples, without re-labeling them (Shorten & Khoshgoftaar, 2019; Jiang et al., 2021). Other techniques construct synthetic examples with modified labels (Lin & Lin, 2023). Motivated by recent studies on multiple complementary-label learning (Cao et al., 2022; Feng et al., 2020), we conjecture that utilizing multiple complementary labels through label sharing has the potential to improve existing CLL models, and thus resort to label-modification techniques. Among such techniques, we choose Mixup (Zhang et al., 2018) because of its natural potential in encouraging complementary-label sharing. While Mixup is well-known for its simplicity and effectiveness, the application of Mixup for CLL remains unexplored prior to our work.

With a wide spectrum of experiments across balanced and imbalanced CLL settings, we confirm that applying Mixup on the complementary labels has the potential to improve various state-of-the-art CLL models by encouraging label sharing, which helps the machine identify the ordinary label more efficiently (Lin & Lin, 2023; Chou et al., 2020b; Yu et al., 2018). But the potential comes with a serious side effect. In particular, sometimes the complementary labels on which Mixup manipulates contains an *ordinary* label of one of the examples, which introduces noise to the label sharing process. The noise significantly deteriorates the performance of the CLL model because of overfitting. The side effect suggests that original Mixup does not work off-the-shelf for CLL.

To mitigate the side effect, we design a novel data augmentation technique called *Intra-Cluster Mixup (ICM)*. ICM clusters the examples before applying Mixup *within each cluster*. The clustering design reduces the noise introduced by Mixup while keeping its potential benefits. Our empirical experiments demonstrate that ICM consistently enhances the CLL performance across a variety of state-of-the-art CLL models and a broad spectrum of settings, ranging from balanced to imbalanced classification. Furthermore, we expand our empirical comparison from 4 common benchmark datasets in existing studies to 7, including both synthetic and real-world labeled datasets. Our efforts significantly broaden the scope of benchmarks in the field. Our unique contributions can be summarized as follows:

- To the best of our knowledge, we are *the first* to introduce a novel data augmentation technique specifically designed for CLL contexts. We identify two critical insights: (i) the original Mixup fails in CLL settings due to noise introduced during the label sharing process, and (ii) mixing samples within the same class proves to be a more effective strategy.
- We propose ICM, a tailored data augmentation technique that addresses the unique challenges of CLL and consistently enhances the performance across various CLL models.
- We conduct extensive benchmarking on large CLL datasets, covering a range from *synthetic* to *real-world* labeled datasets. Our studies span a diverse spectrum of settings, from *balanced* to *imbalanced* CLL, justifying the effectiveness of our framework.

2 Problem Setup

2.1 Complementary-Label Learning

In CLL, we are given a dataset $\bar{D} = \{(\mathbf{x}_i, \bar{y}_i)\}_{i=1}^N$, where each instance $\mathbf{x}_i \in \mathbb{R}^d$ represents an input image, and $\bar{y}_i \in \mathbb{R}^K$ is a complementary label. The complementary label \bar{y}_i indicates a class that the image \mathbf{x}_i does not belong. The dataset consists of N samples, and the goal of CLL is to use this complementary label information to train a classifier. In this context, the complementary label satisfies the condition $\bar{y}_i \in [K] \setminus \{y_i\}$, where y_i is the ordinary label of \mathbf{x}_i , K denotes the total number of classes in the dataset, with $K > 2$. The set $[K] = \{1, 2, \dots, K\}$ represents the set of all possible class labels. This implies that \bar{y}_i is one of the incorrect classes for the instance \mathbf{x}_i . The training set \bar{D} is denoted as $\bar{D} = X \times \bar{Y}$, where X contains the input images and \bar{Y} contains the corresponding complementary labels. In contrast to traditional multi-class classification, where the ordinary label y_i is used to train a classifier, the CLL setup trains the model using the complementary label \bar{y}_i . However, the objective in CLL remains the same: to train a classifier f that accurately predicts the ordinary label y_i for unseen instances. Generally, the classifier f is realized through a decision function $g: \mathbb{R}^d \rightarrow \mathbb{R}^K$, with the classification determined by taking the argmax on g . For example, $f(\mathbf{x}) = \text{argmax}_{k \in [K]} g(\mathbf{x})_k$, where $g(\mathbf{x})_k$ represents the score or confidence that the instance \mathbf{x} belongs to class k . The classifier selects the class with the highest score.

2.2 Recent Approaches of Complementary-Label Learning

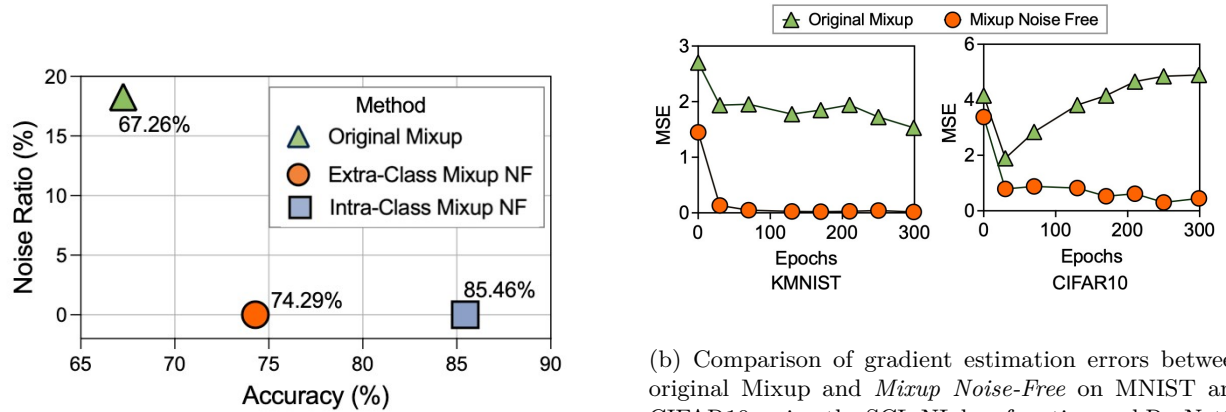
Recent approaches to CLL share a common characteristic: they apply various surrogate loss functions to the standard classifier. For instance, (Ishida et al., 2017; 2019) developed an *unbiased risk estimator (URE)* for arbitrary losses on the standard classifier when employing a uniform transition matrix. When the risk is defined as the classification error, the URE serves as a surrogate metric for performance evaluation. However, UREs are prone to severe negative empirical risks during training, which is indicative of overfitting. To mitigate such overfitting in algorithm design, (Chou et al., 2020b) proposed the *surrogate complementary loss (SCL)*, which is based on minimizing the likelihood associated with complementary label. They justified this approach by showing that SCL constitutes an upper bound to a constant multiple of the standard classification error when the transition matrix is uniform. Another study by (Yu et al., 2018) examined scenarios where the complementary label are not uniformly generated. (Yu et al., 2018) introduced a framework called *forward correction (FWD)* that adapts techniques from noisy label learning (Patrini et al., 2017) to adjust the softmax cross-entropy loss. This is achieved by adding a transition layer to the output of the model: $\bar{f}(\mathbf{x}) = T^T f(\mathbf{x})$, and then utilizing the cross-entropy loss between $\bar{f}(\mathbf{x})$ and the complementary labels \bar{y} . Other research efforts have explored advanced applications beyond single complementary label, including learning from multiple complementary labels (Cao et al., 2022; Feng et al., 2020), and integrating learning from both ordinary and complementary labels (Katsura & Uchida, 2020).

3 Proposed Method

In this section, we propose ICM, a novel data-augmentation technique for CLL. First, we evaluate the performance of the standard Mixup method under various experimental conditions to identify the factors that undermine its effectiveness. Next, we develop enhanced augmentation algorithms that explicitly address these limitations. Finally, we derive and introduce a surrogate complementary-label loss function that seamlessly integrates ICM into the training process.

3.1 Why Mixup does not work?

Applying Mixup naively in the CLL setting results in substantial *complementary-label noise*. This noise arises when the ordinary label appears in the synthetic data generated via original Mixup, thereby violating the core assumption of CLL: $\bar{y}_i \in [K] \setminus y_i$. To empirically verify this claim, we conduct an ablation study measuring the noise ratio introduced by Mixup in a controlled CLL setting. Although CLL typically operates under the assumption that ordinary labels are unavailable or costly to obtain, we adopt a *proof-of-concept* setup where ordinary labels are accessible solely for quantifying the noise. Using the SCL-NL loss (Chou



(a) Relationship between noise ratio and model performance on CIFAR-10 with SCL-NL loss and ResNet18 when applying original Mixup with Mixup Noise-Free (NF) within the same and across different classes.

Figure 1: Analysis of the impact of noise and Mixup Noise-Free (NF) on complementary-label learning performance.

et al., 2020b) and a ResNet18 backbone (He et al., 2016) trained on CIFAR10, we observe that Mixup introduce a noise level of 15.81% (as indicated by the green triangle in Figure 1a). Notably, when training is performed under noise-free conditions, model accuracy improved by 7%, indicating high sensitivity to label noise (highlighted by the orange circle in Figure 1a). These results highlight that label noise in CLL substantially degrades performance. From these observations, we introduce a mathematical framework for analyzing complementary classification error under Mixup augmentation.

Definition 1. Complementary classification error: Let \bar{y}_i denote the complementary hard label (hl) and $\tilde{y}_{i,j}$ the soft label (sl) generated via Mixup. The new input $\tilde{\mathbf{x}}_{i,j}$ is formed by interpolating two training samples \mathbf{x}_i and \mathbf{x}_j : $\tilde{\mathbf{x}}_{i,j} = \lambda \mathbf{x}_i + (1 - \lambda) \mathbf{x}_j$, where $\lambda \in [0, 1] \sim \beta(\alpha, \alpha)$ and i, j index randomly selected examples. Define the loss vector as $\ell(g(\mathbf{x})) = [\ell(1, g(\mathbf{x})), \dots, \ell(K, g(\mathbf{x}))]$. Then:

$$\mathcal{R}_{hl}(g; l) = \frac{1}{N} \sum_{n=1}^N [\ell(\bar{y}_i, g(\mathbf{x}_i))] = \mathbb{E}_{(\mathbf{x}, \bar{y}) \sim \bar{D}} [\bar{y}_i \neq g(\mathbf{x}_i)], \quad (1)$$

$$\mathcal{R}_{sl}(g; \ell) = \frac{1}{N} \sum_{n=1}^N [\ell(\tilde{y}_{i,j}, g(\tilde{\mathbf{x}}_{i,j}))] = \mathbb{E}_{(\mathbf{x}, \bar{y}) \sim \bar{D}} [\bar{y}_i \neq g(\tilde{\mathbf{x}}_{i,j})] + \mathbb{E}_{(\mathbf{x}, \bar{y}) \sim \bar{D}} [\bar{y}_j \neq g(\tilde{\mathbf{x}}_{i,j})]. \quad (2)$$

Definition 2. Error generated by label noise: Given model $f(\mathbf{x})$, the error generated by label noise ε is defined as:

$$\varepsilon = \mathbb{E}_{(\mathbf{x}, \bar{y}) \sim \bar{D}} [\bar{y} = f(\mathbf{x})]. \quad (3)$$

Proposition 1. Complementary error with Mixup: The complementary classification error under Mixup for a synthetic pair $(\tilde{\mathbf{x}}_{i,j}, \tilde{y}_{i,j})$, defined as follows:

$$\mathcal{R}'(g; l) = \frac{1}{N} \sum_{n=1}^N [\ell(\tilde{y}_{i,j}, g(\tilde{\mathbf{x}}_{i,j}))] = \lambda \mathbb{E} [\bar{y}_i \neq g(\tilde{\mathbf{x}}_{i,j})] + (1 - \lambda) \mathbb{E} [\bar{y}_j \neq g(\tilde{\mathbf{x}}_{i,j})] + \lambda \varepsilon_i + (1 - \lambda) \varepsilon_j. \quad (4)$$

Proof. Refer to Appendix A for the proof. \square

The equation 4 emphasizes that minimizing complementary loss under Mixup requires careful control of the noise rate in the generated data. Specifically, it is critical to minimize instances where $\bar{y}_i = y_j \vee \bar{y}_j = y_i$, as such occurrences increase the error term ε in equation 4.

To further explore this effect, we evaluate gradient estimation error under noisy and noise-free setups. Let f denote the true gradient and c the complementary gradient estimator. The estimation error is defined as $\mathbb{E}_{(x,y,\bar{y})}[(f - c)^2]$. As shown in Figure 1b for MNIST and CIFAR10, the error associated with *Mixup Noise-Free* is consistently lower than that of original Mixup, reinforcing that label noise compromises optimization effectiveness.

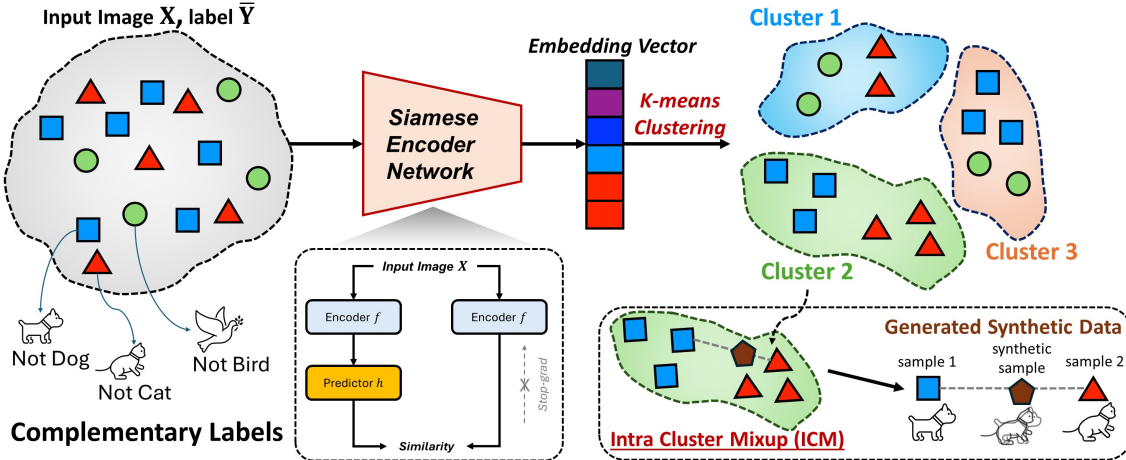


Figure 2: Illustration of the *Intra-Cluster Mixup (ICM)* framework. **Top:** Embedding features are extracted using a pretrained *SimSiam* encoder and clustered using k -means, aiming to group samples with similar ordinary labels. **Bottom right:** Within each cluster, ICM generates synthetic samples by interpolating features and labels, which are then used to train the classifier.

Beyond quantifying noise, we investigate whether the original Mixup strategy used in ordinary learning transfers effectively to the CLL setting. In traditional supervised learning, original Mixup interpolates inputs and labels from different classes, which encourages smooth decision boundaries. In contrast, CLL imposes constraints that make such cross-class interpolation problematic. We hypothesize that mixing data within the same class, termed Intra-Class Mixup, preserves the CLL constraint $\bar{y}_i \in [K] \setminus y_i$ and reduces noise. To evaluate this, we synthetically generate intra-class and extra-class samples under a noise-free setup. Results in Figure 1a (highlighted by the *blue square* and *orange circle*) reveal that *Intra-Class Mixup Noise-Free* outperforms *Extra-Class Mixup Noise-Free* by 11%. This significant margin validates our hypothesis: intra-class mixing is more suitable in the CLL context and significantly improves performance.

The experimental results indicate that original Mixup can be effective under noise-free conditions, eliminating noise typically requires access to ordinary labels which contradicting the fundamental assumption of CLL. To address this challenge, we propose a dedicated framework for CLL, referred to as ICM. This framework is specifically designed to reduce synthetic label noise without requiring knowledge of the ordinary label. The following subsection provides a detailed explanation of the ICM framework.

3.2 Intra-Cluster Mixup in CLL

As discussed in above subsection, we introduce a specialized design for CLL called ICM, illustrated in Figure 2. Our proposed methodology, ICM, comprises two primary components. First, feature representations are extracted from the training data using a self-supervised learning model based on SimSiam (Chen & He, 2021). These embeddings are then clustered using k -means to group samples with similar feature characteristics, as shown in the *top* of Figure 2. This clustering step assigns cluster-based labels to sample and serves as a pre-processing phase. Second, synthetic complementary samples are generated by mixing inputs and

labels within the same cluster, as illustrated in the *bottom right* of Figure 2. These augmented samples are then used to train the classifier. The procedure is defined as:

$$\tilde{\mathbf{x}}_{i,j} = \lambda_{\mathbf{x}} \mathbf{x}_i + (1 - \lambda_{\mathbf{x}}) \mathbf{x}_j \quad (5)$$

$$\tilde{y}_{i,j} = \lambda_{\bar{y}} \bar{y}_i + (1 - \lambda_{\bar{y}}) \bar{y}_j. \quad (6)$$

Integration of ICM into the training process is detailed in Algorithm 1. After clustering the dataset \bar{D} , ICM selects pairs within the same cluster to generate synthetic complementary samples using equation 5 and equation 6. Here, $\lambda_{\mathbf{x}} = \lambda_{\bar{y}}$ is sampled from a beta distribution $\beta(\alpha, \alpha)$, and the selected pairs $(\mathbf{x}_i, \bar{y}_i)$ and $(\mathbf{x}_j, \bar{y}_j)$ are drawn uniformly from the training data.

Algorithm 1: ICM training with cluster-consistent Mixup. Lines 1–3: extract SimSiam embeddings and assign k clusters. Lines 4–12: synthesize $(\tilde{\mathbf{x}}, \tilde{y})$ by interpolating pairs within the same cluster using Eq. (5)–(6). Lines 13–14: update θ on the synthetic batch.

Input: Complementary-labeled dataset $\bar{D} = \{(\mathbf{x}_i, \bar{y}_i)\}_{i=1}^n$, model f_{θ} .

Output: Trained parameters θ .

```

1 (1) Embedding:  $\mathbf{z}_i \leftarrow \mathcal{F}_{\text{sim}}(\mathbf{x}_i)$  for  $i = 1, \dots, n$  //  $\mathcal{F}_{\text{sim}}$ : pretrained SimSiam encoder
2 (2) Clustering: run  $k$ -means on  $\{\mathbf{z}_i\}$  to obtain cluster labels  $c_i \in \{1, \dots, k\}$ .
3 (3) Augment data:  $\bar{D} \leftarrow \{(\mathbf{x}_i, \bar{y}_i, c_i)\}_{i=1}^n$ .
4 while not converged do
5   (4) Sample a minibatch  $\mathcal{B} \subset \bar{D}$ .
6   (5) For each cluster  $u \in \{1, \dots, k\}$ , form  $\mathcal{B}_u = \{(\mathbf{x}, \bar{y}, c) \in \mathcal{B} : c = u\}$ .
7   (6) Initialize synthetic set  $\tilde{\mathcal{B}} \leftarrow \emptyset$ .
8   foreach  $u$  with  $|\mathcal{B}_u| \geq 2$  do
9     for  $m = 1$  to  $M_u$  do
10       Draw two distinct pairs  $(\mathbf{x}_i, \bar{y}_i, u), (\mathbf{x}_j, \bar{y}_j, u) \in \mathcal{B}_u$ . // sampling the samples in same cluster.
11       Sample  $\lambda_{\mathbf{x}} \sim \text{Beta}(\alpha, \alpha)$ .
12       (a) Obtain ICM input  $\tilde{\mathbf{x}}$  using Eq. (5).
13       (b) Compute label mixing coefficient  $\lambda_{\bar{y}}$ .
14       (c) Generate ICM label  $\tilde{y}$  using Eq. (6).
15       Append  $(\tilde{\mathbf{x}}, \tilde{y})$  to  $\tilde{\mathcal{B}}$ .
16   (7) Compute loss:  $\mathcal{L}(\theta) \leftarrow \frac{1}{|\tilde{\mathcal{B}}|} \sum_{(\tilde{\mathbf{x}}, \tilde{y}) \in \tilde{\mathcal{B}}} \mathcal{L}(f_{\theta}(\tilde{\mathbf{x}}), \tilde{y})$ . // training model with new synthetic data.
17   (8) Update:  $\theta \leftarrow \theta - \eta \nabla_{\theta} \mathcal{L}(\theta)$ .
```

Clustering plays a critical role by reducing label noise during data augmentation. Grouping samples within clusters encourages mixing between instances that are more likely to share the same true label. This increases the likelihood that the complementary label condition $\bar{y}_i \in [K] \setminus y_i$ holds across the cluster, thereby reducing the risk of introducing noise.

To evaluate ICM, we conduct an ablation study comparing it with standard Mixup. As shown in Figure 3, ICM significantly reduces the noise ratio. For instance, on MNIST, the ratio drops from 16.24% with Mixup to 0.95% with ICM. The effectiveness of noise reduction correlates with dataset complexity; simpler datasets such as MNIST, KMNIST, and FMNIST exhibit greater improvements than more complex datasets like CIFAR10 and CIFAR20. These results validate the benefit of incorporating clustering into original Mixup for reducing label noise in CLL.

3.3 Surrogate Complementary Loss with ICM

In this subsection, we propose a data augmentation for the existing loss-based CLL algorithms. In CLL, to minimize the non-convex $(0 - 1)$ loss in complementary learning, a common approach in statistical learning is to use a convex surrogate loss to approximate the target loss. In our work, we use ℓ to denote the *surrogate complementary loss (SCL)* loss functions and we combine our proposed data augmentation technique ICM

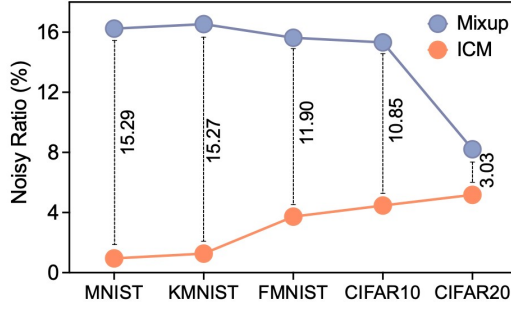


Figure 3: Comparing the noise ratio introduced by Mixup and ICM methods, with a long-tailed *imbalance* ratio $\rho = 100$, SCL-NL loss, and ResNet18 architecture.

with SCL during the training process. The main idea behind ICM data augmentation for complementary labels is to assign a new complementary label and incorporate additional information from samples within the same cluster, which share the same ordinary label. This approach enables the model to access not only more complementary labels but also new information about the samples. Additionally, it helps to reduce the noise that may arise when selecting pairs for data augmentation during training, thereby improving the overall learning process.

In loss-based complementary learning algorithms, a loss function $\ell: [K] \times \mathbb{R}^K \rightarrow \mathbb{R}$ is employed, which takes as input both the complementary label \bar{y}_i and the prediction output of the model $g(\mathbf{x}_i)$. The objective of learning process is to minimize this loss function ℓ over the complementary dataset \bar{D} , which can be formulated as:

$$\mathcal{L}(g_\theta; \ell) = \frac{1}{N} \sum_{i=1}^N \ell\left(\bar{y}_i, g_\theta(\mathbf{x}_i)\right). \quad (7)$$

When incorporating the ICM data augmentation during training, the CLL loss function is updated as follows:

$$\mathcal{L}'(g_\theta; \ell) = \frac{1}{N} \sum_{i=1}^N \ell\left(\tilde{y}_{i,j}, g_\theta(\tilde{\mathbf{x}}_{i,j})\right) = \frac{1}{N} \sum_{i=1}^N \left[\lambda \ell\left(\bar{y}_i, g_\theta(\tilde{\mathbf{x}}_{i,j})\right) + (1 - \lambda) \ell\left(\bar{y}_j, g_\theta(\tilde{\mathbf{x}}_{i,j})\right) \right], \quad (8)$$

where $\lambda \in [0, 1] \sim \beta(\alpha, \alpha)$ (*beta distribution*), for $\alpha \in (0, \infty)$, $\tilde{\mathbf{x}}_{i,j}$ in equation 5, $\tilde{y}_{i,j}$ in equation 6, j is random sampling from the same cluster of i , and N is the size of training dataset. To better distinguish from 0 – 1 based methods, we use a convex surrogate loss to approximate the target loss, denotes ℓ . In fact, previous research in complementary learning has revealed similar patterns focused on minimizing the predictions of label classes, including approaches such as:

- Negative learning loss (SCL-NL) in (Kim et al., 2019): a modified log loss specifically designed for negative learning with complementary labels:

$$\ell_{\text{NL}}(\bar{y}, g(\mathbf{x})) = -\log(1 - \mathbf{p}_{\bar{y}} + \gamma), \text{ where } 0 < \gamma < 1. \quad (9)$$

- Exponential loss (SCL-EXP): $\ell_{\text{EXP}}(\bar{y}, g(\mathbf{x})) = \exp(\mathbf{p}_{\bar{y}}).$ (10)
- Forward correction (FWD) in (Yu et al., 2018) is a method for correcting loss using a forward correction approach based on a given transition matrix T :

$$\ell_{\text{FWD}}(\bar{y}, g(\mathbf{x})) = \ell(\bar{y}, T^T \mathbf{p}). \quad (11)$$

Here, γ is a constant added to the loss function to prevent the SCL-NL loss from approaching infinity when $\mathbf{p}_{\bar{y}}$ equals 1, $\mathbf{p} \in \Delta^{K-1}$ represents the probability output of learning model if g passes through a softmax layer, and Δ^{K-1} is the K -dimensional simplex.

4 Experiments

In this section, we evaluate ICM on synthetic and real-world datasets under both balanced and imbalanced conditions, comparing it with state-of-the-art CLL baselines. Our findings demonstrate that ICM significantly enhances performance and effectively addresses key CLL challenges.

4.1 Experiment Setup

Datasets. We assess the effectiveness of our proposed ICM framework across five synthetic labeled datasets: CIFAR10, CIFAR20, MNIST, KMNIST, and FMNIST. The synthetic labeled datasets consist of CIFAR10 (Krizhevsky et al., 2009) and CIFAR20, each containing 50,000 training samples and 10,000 testing samples. CIFAR10 encompasses 10 classes, whereas CIFAR20 comprises 20 superclasses derived from CIFAR100 (Krizhevsky et al., 2009). We do not benchmark on CIFAR100, as existing CLL algorithms have not demonstrated the ability to learn a meaningful classifier on this dataset when given only one complementary label per data instance. MNIST (Lecun et al., 1998), KMNIST (Clanuwat et al., 2018), and FMNIST (Xiao et al., 2017) each consist of 60,000 training samples and 10,000 testing samples, with all three datasets featuring ten classes.

Additionally, we evaluate our framework on real-world labeled datasets, including CLCIFAR10 and CLCIFAR20 (Wang et al., 2025), which use the images from CIFAR10 and CIFAR20, respectively, with complementary labels annotated by humans. In CLL, MNIST and CIFAR are standard datasets. Researchers have not transitioned to large-scale datasets with numerous classes, such as TinyImageNet (Le & Yang, 2015) and ImageNet (Deng et al., 2009). Preliminary tests reveal that state-of-the-art CLL algorithms struggle to produce meaningful classifiers for 100 classes, even with uniformly and noiselessly generated synthetic complementary labels. This is why existing CLL algorithms are evaluated on datasets with 10, 20 classes.

Table 1: Top-1 validation accuracy ($mean \pm std$) on balanced (bal) $\rho = 1$ and long-tailed imbalanced (imb) ratio $\rho = 10$, K cluster = 50 setups. The methods used are *SCL-NL* (S-NL), *FWD-INT* (FWD), *SCL-EXP* (S-EXP), *DM* losses, and ResNet18. Best performance is *highlighted in bold*.

Method	Imbalanced (imb)		Balanced (bal)	
	CLCIFAR10	CLCIFAR20	CLCIFAR10	CLCIFAR20
S-NL	17.77 \pm 0.20	5.80 \pm 0.03	37.59 \pm 0.40	8.53 \pm 0.24
S-NL+Mix	21.28 \pm 0.51	6.64 \pm 0.48	42.96 \pm 0.54	9.13 \pm 0.44
S-NL+ICM	28.44\pm0.05	7.55\pm0.08	56.63\pm0.61	11.26\pm0.24
DM	15.19 \pm 0.15	5.76 \pm 0.06	38.20 \pm 0.68	8.34 \pm 0.08
DM+Mix	22.99 \pm 0.22	6.92 \pm 0.21	42.61 \pm 0.48	9.12 \pm 0.32
DM+ICM	27.88\pm0.94	7.10\pm0.02	53.04\pm0.40	11.47\pm0.18
FWD	12.07 \pm 0.01	5.98 \pm 0.17	42.98 \pm 0.36	21.10 \pm 0.23
FWD+Mix	17.06 \pm 0.89	6.10 \pm 0.16	42.38 \pm 0.05	21.48 \pm 0.19
FWD+ICM	18.23\pm0.08	7.73\pm0.09	58.97\pm0.21	35.94\pm0.33
S-EXP	17.37 \pm 0.16	5.99 \pm 0.21	41.42 \pm 0.68	8.56 \pm 0.25
S-EXP+Mix	20.38 \pm 0.40	6.84 \pm 0.13	43.56 \pm 0.13	9.04 \pm 0.21
S-EXP+ICM	27.52\pm0.06	7.01\pm0.08	56.26\pm0.15	11.20\pm0.06

Baseline Methods. Our framework can be applied with different methods, we choose SCL-EXP, SCL-NL (Chou et al., 2020b), FWD-INT (Yu et al., 2018), DM (Gao & Zhang, 2021) as our cooperators to validate the efficacy of our approach.

Implementation Details. For a fair comparison, we choose RestNet18 (He et al., 2016) as our backbone. We train the model with a batch size 512 for 300 epochs and an initial learning rate of 10^{-4} , weight decay 10^{-4} , and optimizer Adam. All the experiments were run with Tesla V100-SXM2, 32GB memories. The hyper-parameters can be appropriately tuned via the validation process. For each subtask, we run the experiments three times. Other implemented details, including hyper-parameter selection through validation

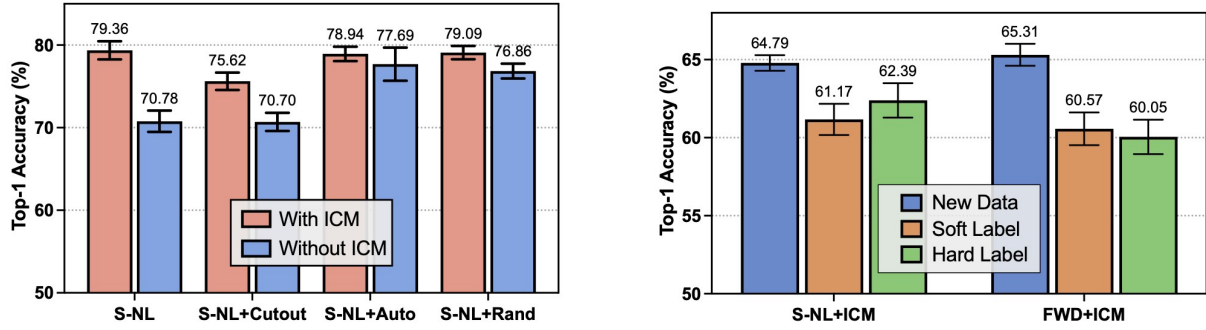
process such as α , K cluster, can be found in our supplementary materials Appendix D. We experiment our proposed method across a wide spectrum of both balanced and imbalanced CLL settings. For imbalanced CLL, we follow (Cao et al., 2019) to generate a long-tailed distribution dataset with different imbalance ratios on ordinary datasets. Details of the different imbalanced setups can be found in the Appendix B.

Table 2: Top-1 validation accuracy ($mean \pm std$) for $\rho = 100$ (long-tailed imbalanced) and $\rho = 1$ (balanced) setups across CIFAR10, CIFAR20, MNIST, KMNIST, and FMNIST datasets using ResNet18 and different loss methods.

Method	CIFAR10		CIFAR20		MNIST		KMNIST		FMNIST	
	$\rho = 100$	$\rho = 1$								
S-NL	22.41 \pm 0.31	65.47 \pm 0.05	10.65 \pm 0.28	24.14 \pm 0.33	50.15 \pm 0.52	97.78 \pm 0.21	35.17 \pm 0.17	88.92 \pm 0.14	51.93 \pm 0.33	85.15 \pm 0.16
S-NL+Mix	31.46 \pm 0.59	67.10 \pm 0.11	13.47 \pm 0.46	26.45 \pm 0.07	54.23 \pm 0.48	96.64 \pm 0.11	37.25 \pm 0.53	79.04 \pm 0.16	56.07 \pm 0.57	84.35 \pm 0.08
S-NL+ICM (ours)	36.21\pm0.19	79.13\pm0.04	18.11\pm0.31	39.17\pm0.15	85.83\pm0.19	98.20\pm0.10	63.70\pm0.34	89.09\pm0.08	67.80\pm0.40	85.25\pm0.99
FWD	22.20 \pm 0.40	64.29 \pm 0.33	8.43 \pm 0.29	23.18 \pm 0.34	50.26 \pm 0.57	97.49 \pm 0.08	35.29 \pm 0.37	80.41 \pm 0.36	51.89 \pm 0.63	84.16 \pm 0.07
FWD+Mix	29.03 \pm 0.39	64.47 \pm 0.26	14.55 \pm 0.46	22.79 \pm 0.06	52.44 \pm 0.49	94.09 \pm 0.37	37.77 \pm 0.47	70.83 \pm 0.11	53.24 \pm 0.48	82.43 \pm 0.59
FWD+ICM (ours)	39.71\pm0.29	79.22\pm0.03	21.76\pm0.26	42.20\pm0.09	85.27\pm0.69	98.18\pm0.10	63.50\pm0.47	88.92\pm0.04	67.90\pm0.47	84.75\pm0.11
DM	20.91 \pm 0.15	58.22 \pm 0.24	10.16 \pm 0.05	21.43 \pm 0.09	51.28 \pm 0.33	95.10 \pm 0.05	32.60 \pm 0.20	73.98 \pm 0.25	49.46 \pm 0.08	82.68 \pm 0.34
DM+Mix	30.52 \pm 0.31	65.78 \pm 0.22	13.27 \pm 0.12	24.95 \pm 0.66	55.78 \pm 2.36	95.69 \pm 0.10	36.37 \pm 1.19	78.15 \pm 0.35	54.22 \pm 0.56	82.77 \pm 0.37
DM+ICM (ours)	36.37\pm0.17	78.64\pm0.05	17.42\pm0.52	38.48\pm0.13	85.91\pm0.15	98.67\pm0.07	66.98\pm4.79	89.60\pm0.52	66.46\pm1.19	84.61\pm0.24
S-EXP	22.96 \pm 0.24	65.84 \pm 0.23	10.13 \pm 0.29	24.07 \pm 0.10	50.29 \pm 0.06	98.68 \pm 0.21	35.62 \pm 0.05	90.38 \pm 0.08	51.30 \pm 0.10	85.23 \pm 0.09
S-EXP+Mix	31.51 \pm 0.18	71.72 \pm 0.29	13.77 \pm 0.17	27.90 \pm 0.25	53.68 \pm 0.28	98.27 \pm 0.12	37.52 \pm 1.02	88.40 \pm 0.23	53.50 \pm 3.53	84.42 \pm 0.21
S-EXP+ICM (ours)	36.70\pm0.10	78.86\pm0.12	16.75\pm0.15	38.91\pm0.22	86.06\pm0.37	98.81\pm0.03	64.46\pm0.04	90.45\pm0.12	64.03\pm3.31	85.73\pm0.20

4.2 Results and Analysis

We compare our results with several baselines, including *without Mixup* and *with Mixup (Mix)*, to verify the efficacy of our proposed method. Additionally, our method can be integrated with various base algorithms such as SCL-NL, FWD-INT, DM, and SCL-EXP.



(a) Enhancing robustness by combining ICM with weak and strong data augmentations techniques on CIFAR10.

(b) Comparison of new, soft, and hard label-sharing strategies under S-NL and FWD losses on CIFAR10.

Figure 4: Experimental results on CIFAR-10: (a) robustness gains from combining ICM with weak and strong data augmentations; (b) performance comparison of new, soft, and hard label-sharing strategies under S-NL and FWD losses.

The results for the real-world labeled datasets, CLCIFAR10 and CLCIFAR20, both in balanced and imbalanced settings with different loss functions, are presented in Table 1. For the synthetic labeled datasets (CIFAR10, CIFAR20, MNIST, KMNIST, and FMNIST) with *setup 1*, spanning from balanced to various imbalance ratios, detailed results are shown in Tables 2. Additional experimental details for *setup 2* and *setup 3*, with varying imbalanced ratios, can be found in Appendix B. Our proposed method consistently outperforms the baselines across all setups, from balanced to imbalanced scenarios, and achieves significant performance improvements when integrated with different base algorithms.

Additionally, we conduct another analyses demonstrating that our proposed method, ICM, proves to be a competitive approach for enhancing CLL. This is evidenced by our assessment of the enhancing robustness of ICM when combining with various data augmentation techniques, ranging from weak (Flipflop, Cutout (De Vries & Taylor, 2017)) to strong (AutoAug (Cubuk et al., 2019), RandAug (Cubuk et al., 2020)). The results in Figure 4a illustrate the significant benefits of combining ICM with various data augmentation techniques, for instance, on the CIFAR10 dataset, the combination of ICM with these augmentations achieves accuracy levels approaching 80%, far surpassing the results of their counterparts without ICM.

Furthermore, we conduct a series of analyses demonstrating that our proposed method, ICM, proves to be a competitive approach for enhancing CLL. This is evidenced by our assessment of the *bias* and *variance* of the empirical *Gradient Analysis* in next section. It is also crucial to highlight that the benefits of sharing new synthetic data extend beyond merely sharing complementary labels in the CLL context. This assertion is supported by an ablation study where we share *new data*, *soft label*, and *hard label* during the model training process. The detailed results presented in Figure 4b. In addition, we propose and investigate methods for mitigating dataset imbalance in CLL, with further empirical findings reported in Appendices C and E.

4.3 Gradient Analysis

We further discuss how the ICM framework gives such improvement by arranging the learning process via gradient analysis. This discussion centers on examining loss gradients within the experimental setup, particularly the *stochastic gradient (SGD)* employed in mini-batch optimization. Specifically, we evaluate the bias-variance tradeoff of the gradient estimation error involving complementary gradients with ICM and the Mixup method versus the ordinary gradient. To provide a more accurate assessment, we utilize the bias-variance decomposition technique. Traditionally used in statistical learning to assess algorithmic complexity, we extend this framework to evaluate the estimation error of the gradient, setting the ordinary gradient as the target. We will show that our proposed framework ICM has a lower *mean squared error (MSE)* than the original Mixup, caused by its slight variance and bias.

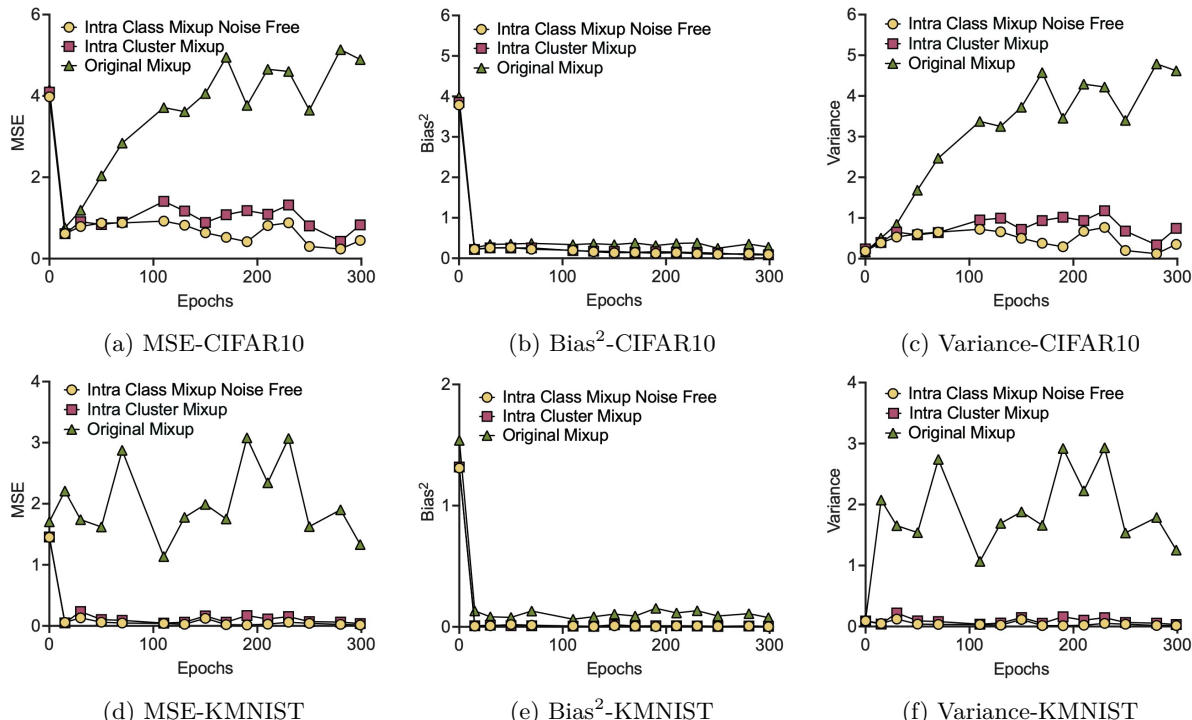


Figure 5: Comparison of gradient estimation errors between original Mixup and *Mixup Noise-Free* on MNIST and CIFAR10, using the SCL-NL loss function and ResNet18 architecture. *Mixup Noise-Free* demonstrates lower gradient estimation error than the original Mixup on both datasets, attributed to reduced noise interference, which impacts classifier performance in CLL contexts.

We represent the gradient step determined by ordinary labeled data (\mathbf{x}, y) and ordinary loss ℓ as f . The complementary gradient step, considering complementary labeled data (\mathbf{x}, \bar{y}) and complementary loss $\bar{\ell}$ or (ϕ) , is denoted as c . Additionally, b denotes the expected gradient step of $[K] \setminus \{y\}$, calculated as the average of c across all possible complementary labels. This can be formalized as follows:

$$f = \nabla \ell(y, g(\mathbf{x})), \quad (12)$$

$$c = \nabla \bar{\ell}(\bar{y}, g(\mathbf{x})), \quad (13)$$

$$b = \frac{1}{K-1} \sum_{y' \neq \bar{y}} \nabla \bar{\ell}(y', g(\mathbf{x})). \quad (14)$$

We designate f as the ground truth, representing the target complementary estimator c . We expect the MSE of the gradient estimation to be minimal.

$$\text{MSE} = \mathbb{E}_{\mathbf{x}, y, \bar{y}}[(f - c)^2]. \quad (15)$$

We drive the bias-variance decomposition by introducing b and eliminating remaining terms:

$$\mathbb{E}[(f - c)^2] = \mathbb{E}[(f - b + b - c)^2], \quad (16)$$

$$= \underbrace{\mathbb{E}[(f - b)^2]}_{\text{Bias}^2} + \underbrace{\mathbb{E}[(b - c)^2]}_{\text{Variance}}. \quad (17)$$

We conduct experiments to assess how well the complementary gradient c approximates the ordinary gradient f and compare it with a baseline method (*original Mixup*). The training process is as follows:

In each epoch, we compute three gradients, namely the ordinary gradient f , the current method c , and b . We evaluate the MSE, the square bias term, and the variance term using equation 15 and equation 17. In each epoch, we update the model only with f to ensure a fair comparison of gradients. The optimizer used was SGD with a learning rate of 10^{-4} , and the training was conducted for 300 epochs.

The results presented in Figure 5 indicate that Mixup exhibits a higher MSE due to elevated levels of variance and bias. Conversely, ICM demonstrates significantly lower variance and bias when compared to Mixup, aligning more closely with the ideal case of *Intra Class Mixup Noise Free*. This supports our observation that our proposed method outperforms Mixup in CLL context by achieving lower variance and bias.

5 Conclusion

This paper presented a novel data augmentation approach, ICM, specifically designs to mitigate the effects of *complementary-label noise* associated with synthetic complementary samples by synthesizing augmented data only within the same cluster. Through rigorous empirical evaluations across diverse CLL settings, we have demonstrated the effectiveness of encouraging complementary label sharing of nearby examples, leading to consistent performance improvements across a wide spectrum of experimental setups, from synthetic to real-world labeled datasets, in both balanced and imbalanced CLL settings. Our empirical experiments reveal that ICM substantially enhances the performance of learning models across a variety of state-of-the-art algorithms. Additionally, our investigations highlight the heightened sensitivity of classifiers trained under CLL conditions to *complementary-label noise*, which leads to performance degradation of CLL models. These findings underscore the significant contribution of ICM to the field of CLL. By providing a data augmentation strategy that effectively tackles the issue of *complementary-label noise*, ICM empowers practitioners to develop more accurate and reliable models in real-world scenarios characterized by CLL.

6 Limitation and Future Works

Despite its contributions, this study has several limitations. First, when applied to simpler models such as linear classifiers and multilayer perceptrons (MLPs) on benchmark datasets such as MNIST, KMNIST, and FMIST, our augmentation technique yields reduced performance. This decline stems from the limited

capacity of these models, which struggle to accommodate the added complexity and increased overlap in feature representations introduced by ICM. Second, we have not yet evaluated our approach in scenarios where instances carry multiple complementary labels. Investigating the benefits of ICM in a multi-complementary-label learning setting remains an important direction for future work.

Broader Impact Statement

We used publicly available benchmarks, including MNIST, KMNIST, FMNIST, CIFAR-10, CIFAR-20, CLCIFAR10, and CLCIFAR20, and identified no significant ethical concerns in their use. To tackle the limited supervision inherent in these datasets, we optimized our learning algorithm to efficiently extract insights from both balanced and imbalanced class distributions. This approach is especially valuable in scientific settings where true labels are sensitive or costly to obtain. Moreover, by relying on complementary labels, we preserve data privacy and reduce annotation costs without sacrificing model accuracy.

References

Kaidi Cao, Colin Wei, Adrien Gaidon, Nikos Arechiga, and Tengyu Ma. Learning imbalanced datasets with label-distribution-aware margin loss. In *Advances in neural information processing systems*, volume 32, 2019. [9](#), [15](#), [16](#), [17](#)

Yuzhou Cao, Shuqi Liu, and Yitian Xu. Multi-complementary and unlabeled learning for arbitrary losses and models. *Pattern Recognition*, 124:108447, 2022. [2](#), [3](#), [16](#)

Xinlei Chen and Kaiming He. Exploring simple siamese representation learning. In *IEEE/CVF Conference on Computer Vision and Pattern Recognition*, pp. 15750–15758, 2021. [5](#)

Hsin-Ping Chou, Shih-Chieh Chang, Jia-Yu Pan, Wei Wei, and Da-Cheng Juan. Remix: rebalanced mixup. In *European Conference on Computer Vision*, pp. 95–110, 2020a. [2](#), [16](#)

Yu-Ting Chou, Gang Niu, Hsuan-Tien Lin, and Masashi Sugiyama. Unbiased risk estimators can mislead: A case study of learning with complementary labels. In *International Conference on Machine Learning*, pp. 1929–1938, 2020b. [2](#), [3](#), [8](#)

Tarin Clanuwat, Mikel Bober-Irizar, Asanobu Kitamoto, Alex Lamb, Kazuaki Yamamoto, and David Ha. Deep learning for classical Japanese literature, 2018. [8](#)

Ekin D Cubuk, Barret Zoph, Dandelion Mane, Vijay Vasudevan, and Quoc V Le. Autoaugment: Learning augmentation strategies from data. In *IEEE/CVF Conference on Computer Vision and Pattern Recognition*, pp. 113–123, 2019. [10](#)

Ekin D Cubuk, Barret Zoph, Jonathon Shlens, and Quoc V Le. Randaugment: Practical automated data augmentation with a reduced search space. In *IEEE/CVF Conference on Computer Vision and Pattern Recognition Workshops*, pp. 702–703, 2020. [10](#)

Yin Cui, Menglin Jia, Tsung-Yi Lin, Yang Song, and Serge Belongie. Class-balanced loss based on effective number of samples. In *IEEE/CVF Conference on Computer Vision and Pattern Recognition*, pp. 9268–9277, 2019. [15](#)

Jia Deng, Wei Dong, Richard Socher, Li-Jia Li, Kai Li, and Li Fei-Fei. Imagenet: A large-scale hierarchical image database. In *IEEE/CVF Conference on Computer Vision and Pattern Recognition*, pp. 248–255, 2009. [8](#)

Terrance DeVries and Graham W. Taylor. Improved regularization of convolutional neural networks with cutout, 2017. URL <https://arxiv.org/abs/1708.04552>. [10](#)

Lei Feng, Takuo Kaneko, Bo Han, Gang Niu, Bo An, and Masashi Sugiyama. Learning with multiple complementary labels. In *International Conference on Machine Learning*, pp. 3072–3081, 2020. [1](#), [2](#), [3](#), [16](#)

Yi Gao and Min-Ling Zhang. Discriminative complementary-label learning with weighted loss. In *International Conference on Machine Learning*, pp. 3587–3597, 2021. 8

Kaiming He, Xiangyu Zhang, Shaoqing Ren, and Jian Sun. Deep residual learning for image recognition. In *IEEE/CVF Conference on Computer Vision and Pattern Recognition*, pp. 770–778, 2016. 4, 8

Takashi Ishida, Gang Niu, Weihua Hu, and Masashi Sugiyama. Learning from complementary labels. In *Advances in Neural Information Processing Systems*, pp. 5639–5649, 2017. 1, 2, 3

Takashi Ishida, Gang Niu, and Masashi Sugiyama. Binary classification from positive-confidence data. In *Advances in Neural Information Processing Systems*, volume 31, 2018. 2, 16

Takashi Ishida, Gang Niu, Aditya Menon, and Masashi Sugiyama. Complementary-label learning for arbitrary losses and models. In *International Conference on Machine Learning*, pp. 2971–2980, 2019. 3

Liming Jiang, Bo Dai, Wayne Wu, and Chen Change Loy. Deceive d: Adaptive pseudo augmentation for gan training with limited data. In *Advances in Neural Information Processing Systems*, pp. 21655–21667, 2021. 2

Rong Jin and Zoubin Ghahramani. Learning with multiple labels. In *Advances in Neural Information Processing Systems*, volume 15, 2002. 1

Yasuhiro Katsura and Masato Uchida. Bridging ordinary-label learning and complementary-label learning. In *Asian Conference on Machine Learning*, pp. 161–176, 2020. 3

Youngdong Kim, Junho Yim, Juseung Yun, and Junmo Kim. Nlnl: Negative learning for noisy labels. In *IEEE/CVF International Conference on Computer Vision*, pp. 101–110, 2019. 7

Alex Krizhevsky, Geoffrey Hinton, et al. Learning multiple layers of features from tiny images. Computer Science University of Toronto, Canada, 2009. 8

Ya Le and Xuan Yang. Tiny imagenet visual recognition challenge. Report of CS231N: Deep Learning for Computer Vision Course, 2015. Stanford University. 8

Y. Lecun, L. Bottou, Y. Bengio, and P. Haffner. Gradient-based learning applied to document recognition. *Proceedings of the IEEE*, 86:2278–2324, 1998. 8

Wei-I Lin and Hsuan-Tien Lin. Reduction from complementary-label learning to probability estimates. In *Pacific-Asia Conference on Knowledge Discovery and Data Mining*, pp. 469–481, 2023. winner of the best paper runner-up award. 2, 16

Agnieszka Mikołajczyk and Michał Grochowski. Data augmentation for improving deep learning in image classification problem. In *International Interdisciplinary PhD Workshop*, pp. 117–122, 2018. 2

Giorgio Patrini, Alessandro Rozza, Aditya Menon, Richard Nock, and Lizhen Qu. Making deep neural networks robust to label noise: a loss correction approach. In *IEEE/CVF Conference on Computer Vision and Pattern Recognition*, pp. 1944–1952, 2017. 3

Sylvestre-Alvise Rebuffi, Sven Gowal, Dan Andrei Calian, Florian Stimberg, Olivia Wiles, and Timothy A Mann. Data augmentation can improve robustness. In *Advances in Neural Information Processing Systems*, pp. 29935–29948, 2021. 2

Jiawei Ren, Cunjun Yu, Xiao Ma, Haiyu Zhao, Shuai Yi, et al. Balanced meta-softmax for long-tailed visual recognition. In *Advances in Neural Information Processing Systems*, pp. 4175–4186, 2020. 16

Connor Shorten and Taghi M Khoshgoftaar. A survey on image data augmentation for deep learning. *Journal of Big Data*, 6:1–48, 2019. 2

Hsiu-Hsuan Wang, Mai Tan Ha, Nai-Xuan Ye, Wei-I Lin, and Hsuan-Tien Lin. CLImage: Human-annotated datasets for complementary-label learning. *Transactions on Machine Learning Research*, 2025. ISSN 2835-8856. 8

Han Xiao, Kashif Rasul, and Roland Vollgraf. Fashion-MNIST: a novel image dataset for benchmarking machine learning algorithms, 2017. [8](#)

Xiyu Yu, Tongliang Liu, Mingming Gong, and Dacheng Tao. Learning with biased complementary labels. In *European Conference on Computer Vision*, pp. 68–83, 2018. [2](#), [3](#), [7](#), [8](#), [16](#)

Hongyi Zhang, Moustapha Cisse, Yann N. Dauphin, and David Lopez-Paz. mixup: Beyond empirical risk minimization. In *International Conference on Learning Representations*, 2018. [2](#)

Zhi-Hua Zhou. A brief introduction to weakly supervised learning. *National Science Review*, 5:44–53, 08 2017. ISSN 2095-5138. [1](#)

Appendix

A Proof

Proof. **Proposition 1** The data augmentation $(\tilde{\mathbf{x}}_{i,j}, \tilde{y}_{i,j})$, generated by $\tilde{\mathbf{x}}_{i,j} = \lambda \mathbf{x}_i + (1 - \lambda) \mathbf{x}_j$, $\tilde{y}_{i,j} = \lambda \bar{y}_i + (1 - \lambda) \bar{y}_j \in \mathbb{R}^K$, is a new data mixture using the original Mixup under CLL. Here, \bar{y}_n is a one-hot encoded with K-dim. The introduction of noise in the new data augmentation occurs if and only if $P(\bar{y}_i = y_j) \vee P(\bar{y}_j = y_i)$, where i and j denote the selected pairs for mixing new data. The degree of noise during the generalization of new data within the original Mixup framework is denoted as ε :

$$\varepsilon_n = \mathbb{E}_{(\mathbf{x}, \bar{y}) \sim \bar{D}} [\bar{y} = f(\mathbf{x})]$$

The complementary classification error, when we employ Mixup, can be obtained by:

$$\begin{aligned} \mathcal{R}'(g; l) &= \frac{1}{N} \sum_{n=1}^N [\ell(\tilde{y}_{i,j}, g(\tilde{\mathbf{x}}_{i,j}))] \\ &= \frac{\lambda}{N} \sum_{n=1}^N [\ell(\bar{y}_i, g(\tilde{\mathbf{x}}_{i,j}))] + \frac{1-\lambda}{N} \sum_{j=1}^N [\ell(\bar{y}_j, g(\tilde{\mathbf{x}}_{i,j}))] \\ &= \lambda \mathbb{E}_{(\tilde{\mathbf{x}}_{i,j}, \bar{y}_i) \sim \bar{D}} [\bar{y}_i \neq g(\tilde{\mathbf{x}}_{i,j})] + \lambda \mathbb{E}_{(\tilde{\mathbf{x}}_{i,j}, \bar{y}_i) \sim \bar{D}} [\bar{y}_i = g(\tilde{\mathbf{x}}_{i,j})] \\ &\quad + (1-\lambda) \mathbb{E}_{(\tilde{\mathbf{x}}_{i,j}, \bar{y}_j) \sim \bar{D}} [\bar{y}_j \neq g(\tilde{\mathbf{x}}_{i,j})] + (1-\lambda) \mathbb{E}_{(\tilde{\mathbf{x}}_{i,j}, \bar{y}_j) \sim \bar{D}} [\bar{y}_j = g(\tilde{\mathbf{x}}_{i,j})] \\ &= \lambda \mathbb{E}_{(\tilde{\mathbf{x}}_{i,j}, \bar{y}_i) \sim \bar{D}} [\bar{y}_i \neq g(\tilde{\mathbf{x}}_{i,j})] + (1-\lambda) \mathbb{E}_{(\tilde{\mathbf{x}}_{i,j}, \bar{y}_j) \sim \bar{D}} [\bar{y}_j \neq g(\tilde{\mathbf{x}}_{i,j})] + \lambda \varepsilon_i + (1-\lambda) \varepsilon_j \end{aligned}$$

□

B Generating Imbalanced Complementary Labels

In this section, we specifically consider three situations as the primary causes of imbalanced complementary labels:

Setup 1: Imbalanced ordinary with a uniform transition matrix

In this configuration, the imbalance in the ordinary distribution dataset results in a corresponding imbalance in complementary labels. The ratio of imbalance in complementary labels significantly decreases compared to the ordinary distribution (e.g., from 100 to around 1.4) when generated using a uniform transition matrix. This imbalance generation is visually represented as *setup 1* in Figure 6a.

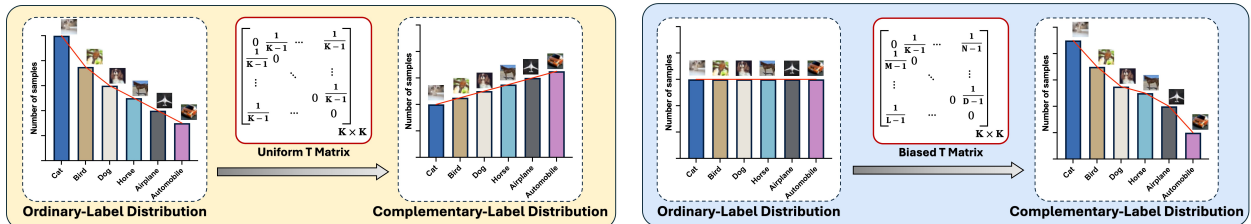
Setup 2: Balanced ordinary with a biased transition matrix

Here, a biased transition matrix arises from the imbalance in complementary labels, as depicted in (b) *setup 2* in Figure 6b, where complementarity probabilities vary across classes. The imbalance in complementary labels aligns with the observed imbalance ratio in the transition matrix (e.g., both being 10). This correlation underscores the direct influence of complementary label distribution on the imbalance characteristics of the transition matrix in this setting.

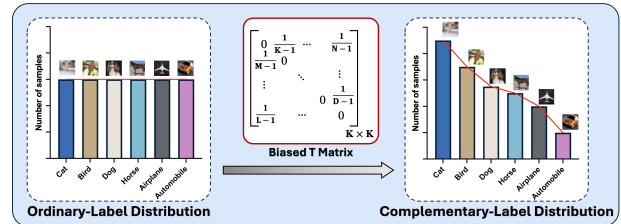
Setup 3: Imbalanced both ordinary and biased transition matrix

The imbalance in both ordinary and biased transition matrix compounds the challenge in CLL. This setup intensifies the bias in complementary labels compared to the previous setups. *setup 3* is particularly challenging for the model to find a good classifier f due to the under-representation of minority classes. Figure 6c illustrates the generation of imbalanced complementary labels in *setup 3*.

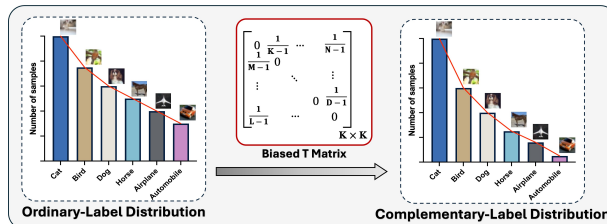
In our proposed setup, we introduce a setting of *long-tailed imbalance*, a concept seen in previous works (Cao et al., 2019; Cui et al., 2019). This setup is designed to generate both an imbalanced ordinary distribution and



(a) Setup 1: Imbalanced ordinary with a uniform transition matrix



(b) Setup 2: Balanced ordinary with a biased transition matrix



(c) Setup 3: Imbalanced both ordinary and biased transition matrix

Figure 6: Illustration of the generation of imbalanced complementary label settings.

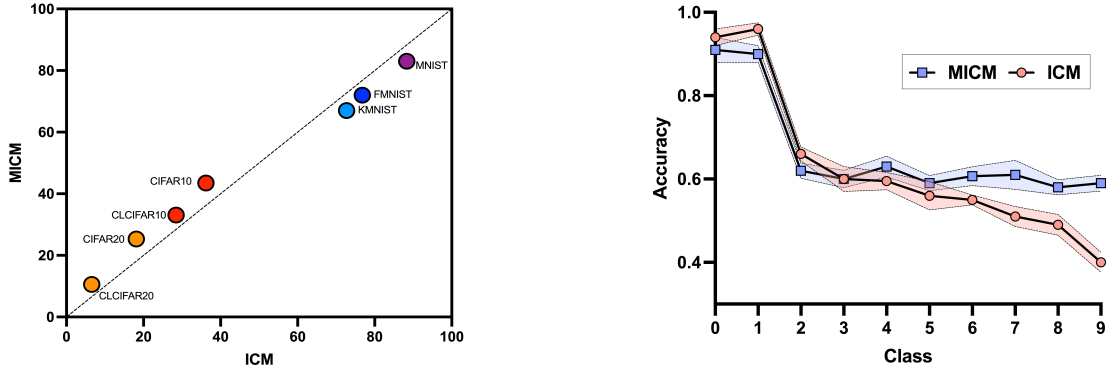
a biased transition matrix. The degree of *long-tailed imbalance* is characterized by the parameter ρ , which dictates class sizes through an exponentially decreasing sequence. The decreasing constant, represented as $\rho^{1/K-1}$, precisely controls the class imbalance ratio of ρ . To illustrate, consider an example of a long-tailed ordinary distribution in *setup 1*, visualized in Figure 6a.

C Imbalanced issue in Complementary-Label Learning

The most prevalent assumption in CLL is uniform generation, positing that complementary labels are generated from ordinary labels with equal probability (Cao et al., 2022; Feng et al., 2020; Lin & Lin, 2023; Ishida et al., 2018). Another research has delved into the non-uniform generation of complementary labels (Yu et al., 2018). However, regardless of whether the assumptions are uniform or non-uniform, existing benchmark datasets generally contain roughly balanced portions of complementary labels.

To the best of our knowledge, no one has explored *what strategies should be adopted when dealing with thousands of complementary labels that are highly imbalanced?* This gap in the literature motivates our study, which aims to explore and develop potential methodologies for addressing the issue of imbalances in CLL datasets. Imbalanced CLL may arise due to an uneven distribution in the ordinary dataset or an imbalanced transition matrix employed for generating complementary labels. In this study, we specifically consider three situations as the primary causes of imbalanced complementary labels: *setup 1*: Imbalance in ordinary with a uniform transition matrix, *setup 2*: Balanced ordinary with a biased transition matrix, and *setup 3*: Imbalance in both ordinary and a biased transition matrix. The illustration of 3 setups in detail is depicted in Appendix B.

In the Mixup, the mixing factor λ_x remains the same for synthetic \mathbf{x} and \bar{y} , i.e., $\lambda_x = \lambda_{\bar{y}}$. However, a significant challenge in imbalanced classification is that minority classes are under-represented in the objective function, leading to poor generalization for these classes by the classifier (Cao et al., 2019; Ren et al., 2020). To address this issue, it is crucial to develop methods that enhance model learning for minority classes. Inspired by a successful Mixup variant that enhances class-imbalanced learning by making y not uniform (Chou et al., 2020a) and recognizing the essential need for sharing more complementary labels among minority classes, we propose *Multi Intra-Cluster Mixup (MICM)*. MICM extends the mixing of samples within the same cluster when generating new synthetic data, thereby encouraging more complementary



(a) Effectiveness of ICM vs MICM on different complementary datasets. The figure reveals that MICM outperforms on complex datasets like CIFAR and CLCIFAR, while ICM proves to be more efficient on simpler datasets, such as the MNIST family.

(b) Comparison of MICM vs ICM in imbalanced CLL on CIFAR10. This ablation study demonstrates that MICM not only achieves better overall performance in imbalanced CLL scenarios but also significantly enhances model learning for minority classes.

Figure 7: The illustration of ablation study on different setups.

label sharing for minority classes. To verify this hypothesis, we conducted an ablation study comparing the effects of MICM versus ICM on enhancing the learning of minority classes in imbalanced CLL. This study was performed on setup 1, with an imbalance ratio $\rho = 10$, utilizing the SCL-NL loss function and the ResNet18 architecture. The results, as shown in Figure 7b, confirm that MICM improves the learning model in minority classes, thereby demonstrating its efficacy in imbalanced CLL. In MICM, we calculate $\lambda_{\bar{y}}$ based on *Inverse Distance Weighting (IDW)*. The core concept of IDW involves determining $\lambda_{\bar{y}}$ based on the distances among randomly selected samples in the cluster. For instance, when three samples are randomly chosen within a cluster, the new sample will be generated by equation 18, then this one serves as an anchor to calculate distances to the other three; the sample closer to the anchor is assigned a higher weight than the farther sample. The formulation for MICM is as follows:

$$\tilde{\mathbf{x}}_{i,j,k} = \lambda_1 \mathbf{x}_i + \lambda_2 \mathbf{x}_j + \lambda_3 \mathbf{x}_k, \quad (18)$$

$$\tilde{y}_{i,j,k} = \lambda_{\bar{y}_1} \bar{y}_i + \lambda_{\bar{y}_2} \bar{y}_j + \lambda_{\bar{y}_3} \bar{y}_k. \quad (19)$$

Note that $\lambda_1, \lambda_2, \lambda_3 \in [0, 1] \sim Dir(\alpha, \alpha, \alpha)$ (*dirichlet distribution*), whereas we compute $\lambda_{\bar{y}}$ for MICM based on the following formulas equation 20, where $\lambda_{\bar{y}} \in [0, 1]$ and $d(\tilde{\mathbf{x}}, \mathbf{x}_i)$ is Euclidean distance between anchor and sample i-th.

$$\lambda_{\bar{y}_i} = \frac{1}{\sum_{i=1}^3 \frac{1}{d(\tilde{\mathbf{x}}, \mathbf{x}_i)}} \quad \text{where, } d(\tilde{\mathbf{x}}, \mathbf{x}_i) = \begin{cases} C, & \text{if } \|\tilde{\mathbf{x}} - \mathbf{x}_i\|_2 = 0, \\ \|\tilde{\mathbf{x}} - \mathbf{x}_i\|_2, & \text{otherwise.} \end{cases} \quad (20)$$

Using Algorithm 1, our proposed MICM method obtains mixed input based on equation 18, mixed labels according to equation 19, and computes $\lambda_{\bar{y}}$ using equation 20. The hyperparameter C plays a crucial role; it is introduced to prevent a 0 value and offers flexibility in controlling the weight of $\lambda_{\bar{y}}$. Specifically, when C is small, the weight of the anchor becomes more substantial, and conversely, when C is large, the weight of the anchor diminishes. The fine-tuning of C spectrum value is provided in *Parameterization* subsection.

D Additional Results of Ablation Study

D.1 Comparing ICM vs. MICM in Imbalanced CLL

For imbalanced CLL, we follow (Cao et al., 2019) to generate a long-tailed distribution dataset with different imbalance ratios ρ (10, 100) on ordinary datasets for *setup 1*. For *setup 2*, we use the same method as (Cao

et al., 2019) to generate a biased transition matrix with imbalance ratios ρ (3, 5, 10). In *setup 3*, we combine both long-tailed distributions on ordinary datasets with imbalance ratios ρ (10, 50, 100) and a biased transition matrix with imbalance ratios ρ (5, 10). The details of the experiment on five synthetic labeled datasets with these three setups and two real-world labeled datasets are presented in next subsection.

An intriguing observation is that while multiple Mixup augmentation may introduce significant noise (*cons*), its regularization effect (*pros*) may not be necessary for simpler tasks. This contrast makes the MICM method less effective than ICM on the MNIST family datasets.

However, for the more complex CIFAR datasets, the MICM method becomes preferable, as shown in Figure 7a, which compares the effectiveness of ICM and MICM on different complementary datasets. In imbalanced CLL scenarios, MICM also demonstrates superiority by more effectively enhancing learning in minority classes and improving overall model performance. Detailed results supporting this finding can be found in Figure 8b.

D.2 Quantifying Model Performance: Mixup within the Same Complementary-Label vs. Intra-Cluster Mixup

To assess the model performance of Mixup within the same complementary-label and ICM, we conduct experiments on five datasets using *setup 1*. The configurations include a long-tailed imbalance ratio $\rho = 100$, $K = 50$, utilizing *SCL-NL* loss function, and the ResNet18 architecture. The results, presented in Figure 8a, clearly demonstrate a significant performance improvement with ICM compared to Mixup within the same complementary-label across all five datasets. These findings validate the superiority of our proposed method, ICM, over the Mixup within the same complementary-label approach.

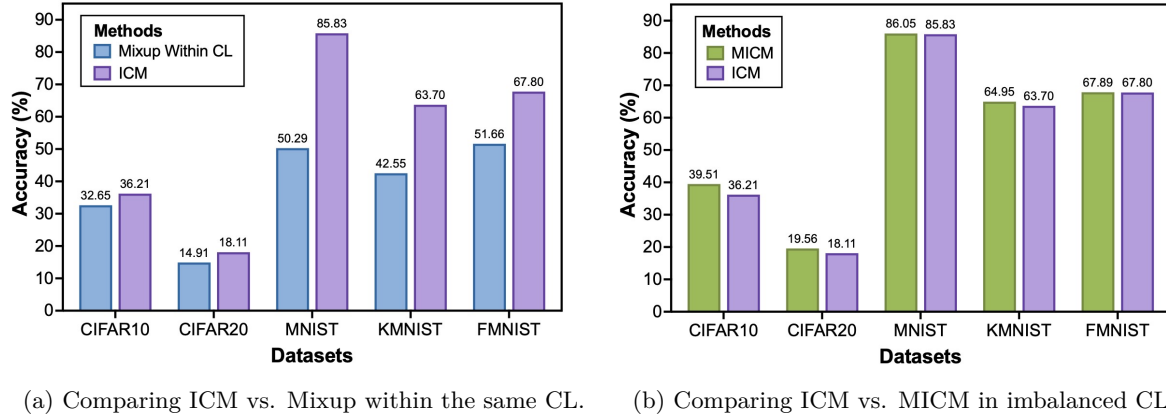


Figure 8: Ablation study comparing our proposed ICM method with other Mixup variants using the S-NL method under Setup 1 with imbalance ratio $\rho = 100$ and ResNet18 architecture.

D.3 Extra-Class Mixup Filter vs. Intra-Class Mixup Filter under Imbalanced CLL Setting

In this section, we perform an ablation study to compare the performance of models using Intra-Class Mixup Filter and Extra-Class Mixup Filter. This analysis aims to elucidate the advantages of Intra and Extra Mixup under the CLL scenario. We conduct experiments on CIFAR10 dataset using *setup 1*. The configurations include a long-tailed imbalance ratio $\rho = 100$, $K = 50$, SCL-NL loss, and the ResNet18 architecture. The results presented in Table 3 demonstrate a significant superiority of Intra-Class Mixup over Extra-Class Mixup in the CLL setting.

Table 3: Comparison of Extra-Class Mixup filter and Intra-Class Mixup filter in CLL setting with *setup 1* a long-tailed imbalance (*imb*) ratio $\rho = 100$, $K = 50$, SCL-NL loss, on CIFAR10 dataset, and ResNet18 architecture

	Noise Ratio	Accuracy
Extra-Class Mixup Filter	0%	37.17 ± 0.30
Intra-Class Mixup Filter	0%	48.59 ± 0.40

D.4 Parameterization

D.4.1 Fine-tuning α Hyper-parameter

We conduct an ablation study to optimize the selection of the α parameter across five datasets: CIFAR10, CIFAR20, MNIST, KMNIST, and FMNIST. The study systematically explores a range from 0 to 2.0 to investigate the performance of different values of α . The optimal α values, identified based on the outcomes of this study, are summarized in Table 4. Notably, the chosen α values for MNIST and KMNIST remain consistent across both the beta and dirichlet distributions, while those for CIFAR10, CIFAR20, and FMNIST varied between the two distributions.

Table 4: Selected α for beta distribution $\beta(\alpha, \alpha)$ and dirichlet distribution $Dir(\alpha, \alpha, \alpha)$

Dataset	$\beta(\alpha, \alpha)$	$Dir(\alpha, \alpha, \alpha)$
CIFAR10	0.4	0.2
CIFAR20	0.1	0.4
MNIST	0.1	0.1
KMNIST	0.3	0.3
FMNIST	0.1	0.4

D.4.2 Fine-tuning K Cluster Hyper-parameter

Another ablation study aims to optimize the selection of the K cluster hyper-parameter across the same five datasets. This study focuses on the *S-NL+ICM* method under *setup 1* with an imbalance ratio $\rho = 100$ and ResNet 18 architecture. The exploration spans a range from 30 to 90, and the results, presented in Figure 9, lead to the selection of $K = 50$ for all five datasets. This choice balances performance metrics and computational efficiency, offering reasonable performance and practicality in terms of training time.

D.4.3 Fine-tuning C Constant Value

We conduct an ablation study to optimize the selection of the C value across the same five datasets. This study focuses on the *S-NL+MICM* method under *setup 1* with an imbalance ratio $\rho = 100$ and ResNet18 architecture. The exploration covers a range from 10 to 50, systematically assessing the performance across various values of C uses for IDW. Detailed results for different C values are presented in Figure 9. We choose $C = 30$ for all five datasets based on its overall performance across the datasets.

E Additional Results of the Experiments

In this section, we conduct additional experiments to cover the remaining datasets CIFAR10, CIFAR20 of *setup 1* and all remaining imbalance types from *setup 2* to *setup 3*. Tables 5 and 6 present the results for *setup 2* with imbalance ratios (*biased transition matrix*) $\rho = (3, 5, 10)$, while Tables 7 and 8 report the results for *setup 3*, which combines a biased transition matrix $\rho = (5, 10)$ with an ordinary imbalance distribution $\rho = (10, 50, 100)$. These findings consistently affirm that our proposed method outperforms

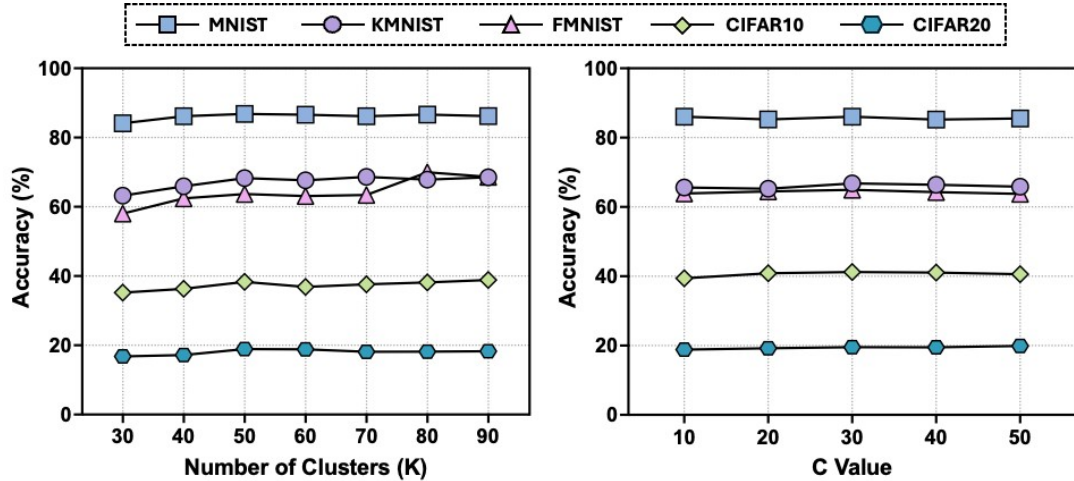


Figure 9: Ablation study analyzing the relationship between model performance and the number of clusters K (left) and the C value (right) across multiple datasets, using the S-NL+ICM method under *setup 1* with imbalance ratio $\rho = 100$ and ResNet18 architecture.

other approaches, demonstrating superiority with SCL-NL, SCL-EXP, FWD-INT and DM loss functions across various imbalance settings.

Based on these experimental results, we propose utilizing ICM for simpler vision datasets such as MNIST, KMNIST, and FMNIST. For more complex vision datasets, including CIFAR10, CLCIFAR10, CIFAR20, and CLCIFAR20, MICM method is preferable to enhance the performance of the trained classifier.

Table 5: Top-1 validation accuracy ($mean \pm std$) on *setup 2* with biased transition ratio $\rho = \{3, 5, 10\}$, $K = 50$, using S-NL, FWD, DM, and S-EXP losses on ResNet18 architecture

Dataset	CIFAR-10			CIFAR-20		
	$\rho = 10$	$\rho = 5$	$\rho = 3$	$\rho = 10$	$\rho = 5$	$\rho = 3$
S-NL	15.49 \pm 0.24	19.08 \pm 0.27	22.10 \pm 0.30	6.70 \pm 0.20	7.09 \pm 0.39	8.16 \pm 0.26
S-NL+Mix	20.74 \pm 0.44	28.03 \pm 0.32	33.71 \pm 0.38	7.21 \pm 0.36	9.83 \pm 0.27	10.49 \pm 0.45
S-NL+ICM	24.68 \pm 0.42	33.97 \pm 0.47	40.57 \pm 0.45	7.36 \pm 0.31	10.25 \pm 0.25	10.65 \pm 0.34
S-NL+MICM	26.16\pm0.26	34.96\pm0.31	42.66\pm0.36	8.73\pm0.27	11.97\pm0.39	14.81\pm0.23
FWD	57.57 \pm 0.56	58.82 \pm 0.47	60.80 \pm 0.40	21.81 \pm 0.31	21.63 \pm 0.28	22.12 \pm 0.29
FWD+Mix	64.10 \pm 0.39	65.05 \pm 0.49	64.94 \pm 0.56	19.38 \pm 0.37	22.03 \pm 0.39	21.21 \pm 0.28
FWD+ICM	78.97 \pm 0.68	78.74 \pm 0.47	78.70 \pm 0.65	35.53 \pm 0.43	37.34 \pm 0.51	39.43 \pm 0.55
FWD+MICM	80.00\pm0.55	80.61\pm0.36	80.70\pm0.63	42.82\pm0.61	45.70\pm0.37	45.67\pm0.52
DM	15.30 \pm 0.28	16.04 \pm 0.33	18.69 \pm 0.32	6.13 \pm 0.17	6.32 \pm 0.34	6.81 \pm 0.33
DM+Mix	26.15 \pm 0.32	29.89 \pm 0.28	33.28 \pm 0.52	6.60 \pm 0.19	8.17 \pm 1.36	9.78 \pm 0.35
DM+ICM	29.78 \pm 0.08	36.94 \pm 0.21	39.24 \pm 0.14	7.06 \pm 0.12	8.53 \pm 0.21	10.16 \pm 0.25
DM+MICM	31.06\pm0.09	39.47\pm0.12	41.40\pm0.21	8.04\pm0.16	10.68\pm0.24	13.84\pm0.21
S-EXP	15.52 \pm 0.31	18.51 \pm 0.29	21.79 \pm 0.25	6.44 \pm 0.21	7.00 \pm 0.23	7.39 \pm 0.24
S-EXP+Mix	20.99 \pm 0.23	27.40 \pm 0.27	31.06 \pm 0.56	7.94 \pm 0.43	9.37 \pm 0.67	11.18 \pm 0.37
S-EXP+ICM	24.30 \pm 0.06	33.45 \pm 0.20	40.36 \pm 0.22	7.03 \pm 0.27	10.14 \pm 0.14	10.56 \pm 0.03
S-EXP+MICM	25.34\pm0.08	34.35\pm0.14	41.56\pm0.19	8.27\pm0.10	10.68\pm0.12	14.44\pm0.09

Table 6: Top-1 validation accuracy ($mean \pm std$) on *setup 2* with biased transition imbalance ratio $\rho = (3, 5, 10)$, $K = 50$, using S-NL, FWD, DM, and S-EXP losses with ResNet18 architecture

Dataset	MNIST		KMNIST		FMNIST	
	$\rho = 10$	$\rho = 5$	$\rho = 10$	$\rho = 5$	$\rho = 10$	$\rho = 5$
Method ρ						
S-NL	57.19 \pm 0.38	66.47 \pm 0.46	28.70 \pm 0.44	41.41 \pm 0.36	46.88 \pm 0.54	67.73 \pm 0.32
S-NL+Mix	35.77 \pm 0.37	53.30 \pm 0.35	23.42 \pm 0.47	31.40 \pm 0.45	34.95 \pm 0.41	48.37 \pm 0.36
S-NL+ICM	77.27 \pm 0.72	97.99\pm0.68	54.84 \pm 0.42	65.37\pm0.38	50.00 \pm 0.39	64.06 \pm 0.62
S-NL+MICM	95.67\pm0.56	96.99 \pm 0.63	63.19\pm0.39	64.11 \pm 0.46	54.98\pm0.57	67.28\pm0.62
FWD	93.00 \pm 0.41	94.46 \pm 0.59	65.67 \pm 0.56	73.97 \pm 0.37	80.60 \pm 0.42	83.51 \pm 0.58
FWD+Mix	88.70 \pm 0.37	92.29 \pm 0.46	63.88 \pm 0.43	68.30 \pm 0.39	78.37 \pm 0.38	80.13 \pm 0.31
FWD+ICM	98.15\pm0.45	98.21\pm0.35	88.09\pm0.68	87.75\pm0.47	85.95\pm0.54	85.80\pm0.48
FWD+MICM	98.00 \pm 0.42	98.08 \pm 0.78	86.87 \pm 0.37	87.50 \pm 0.41	85.02 \pm 0.23	85.48 \pm 0.57
DM	46.95 \pm 0.32	70.38 \pm 0.30	27.84 \pm 0.41	32.71 \pm 0.31	43.57 \pm 0.39	54.03 \pm 0.42
DM+Mix	35.39 \pm 0.34	50.74 \pm 0.36	26.06 \pm 0.52	29.27 \pm 0.58	39.56 \pm 0.54	45.90 \pm 0.49
DM+ICM	86.96 \pm 0.12	97.01\pm0.11	63.65\pm0.23	65.46\pm0.21	52.42 \pm 0.18	70.61\pm0.08
DM+MICM	92.99\pm0.14	94.85 \pm 0.15	58.24 \pm 0.21	60.43 \pm 0.17	59.45\pm0.18	68.25 \pm 0.12
S-EXP	57.21 \pm 0.25	65.84 \pm 0.28	28.71 \pm 0.41	41.88 \pm 0.43	46.08 \pm 0.52	56.65 \pm 0.34
S-EXP+Mix	27.91 \pm 0.43	36.71 \pm 0.45	22.16 \pm 0.49	32.02 \pm 0.72	43.95 \pm 0.68	40.44 \pm 0.56
S-EXP+ICM	69.11 \pm 0.11	97.70 \pm 0.19	54.26 \pm 0.16	66.80\pm0.19	48.21 \pm 0.14	63.32 \pm 0.21
S-EXP+MICM	87.12\pm0.18	97.92\pm0.13	62.49\pm0.23	64.55 \pm 0.16	56.38\pm0.20	66.47\pm0.13

Table 7: Top-1 validation accuracy ($mean \pm std$) on *setup 3* combining biased transition ratio $\rho_1 = 5$ and long-tailed imbalance $\rho_2 = (10, 50, 100)$, $K = 50$, using S-NL, FWD, DM, S-EXP losses and ResNet18.

Datatset	MNIST			CIFAR-10		
	5, 100	5, 50	5, 10	5, 100	5, 50	5, 10
Method ρ_1, ρ_2						
S-NL	39.18 \pm 0.33	41.49 \pm 0.37	51.76 \pm 0.58	16.16 \pm 0.39	14.84 \pm 0.37	12.96 \pm 0.36
S-NL+Mix	37.38 \pm 0.35	37.89 \pm 0.37	47.90 \pm 0.39	16.00 \pm 0.45	15.39 \pm 0.38	17.15 \pm 0.46
S-NL+ICM	89.44 \pm 0.43	94.55\pm0.42	97.41\pm0.42	18.89 \pm 0.49	21.00 \pm 0.38	19.81 \pm 0.45
S-NL+MICM	90.08\pm0.46	93.72 \pm 0.51	96.80 \pm 0.36	20.98\pm0.51	22.87\pm0.42	32.78\pm0.54
FWD	47.93 \pm 0.34	54.02 \pm 0.42	64.03 \pm 0.30	22.18 \pm 0.56	23.67 \pm 0.47	23.94 \pm 0.31
FWD+Mix	46.98 \pm 0.31	51.23 \pm 0.43	67.42 \pm 0.48	30.20 \pm 0.48	29.77 \pm 0.43	38.68 \pm 0.45
FWD+ICM	85.34\pm0.48	93.91\pm0.41	97.15\pm0.53	37.74 \pm 0.36	40.34 \pm 0.51	64.06 \pm 0.42
FWD+MICM	83.49 \pm 0.41	91.69 \pm 0.49	95.79 \pm 0.57	40.78\pm0.43	43.71\pm0.39	65.33\pm0.37
DM	36.91 \pm 0.29	36.25 \pm 0.51	48.57 \pm 0.39	14.04 \pm 0.41	14.62 \pm 0.35	14.40 \pm 0.28
DM+Mix	34.85 \pm 0.32	40.68 \pm 0.29	46.62 \pm 0.43	18.26 \pm 0.38	19.36 \pm 0.54	18.37 \pm 0.72
DM+ICM	88.13\pm0.12	91.38\pm0.21	96.75\pm0.15	21.17 \pm 0.13	22.43 \pm 0.07	32.55 \pm 0.09
DM+MICM	81.66 \pm 0.23	84.98 \pm 0.15	92.73 \pm 0.11	22.48\pm0.17	23.95\pm0.16	32.61\pm0.10
S-EXP	40.57 \pm 0.32	40.46 \pm 0.35	44.79 \pm 0.30	15.68 \pm 0.38	14.45 \pm 0.27	12.80 \pm 0.36
S-EXP+Mix	34.52 \pm 0.41	36.08 \pm 0.43	42.28 \pm 0.52	15.58 \pm 0.45	14.13 \pm 0.57	16.58 \pm 0.51
S-EXP+ICM	80.52 \pm 0.09	84.18 \pm 0.13	98.13\pm0.17	18.25 \pm 0.20	19.78 \pm 0.17	20.30 \pm 0.16
S-EXP+MICM	83.17\pm0.16	85.11\pm0.21	97.82 \pm 0.08	19.26\pm0.19	20.43\pm0.11	31.32\pm0.23

Table 8: Top-1 validation accuracy ($mean \pm std$) on *setup 3* combining biased transition ratio $\rho_1 = 10$ and long-tailed imbalance $\rho_2 = (10, 50, 100)$, with $K = 50$, using S-NL, FWD, DM, S-EXP losses and ResNet18 architecture

Datatset	MNIST			CIFAR-10		
	10, 100	10, 50	10, 10	10, 100	10, 50	10, 10
Method ρ_1, ρ_2						
S-NL	38.01 \pm 0.40	41.19 \pm 0.38	43.52 \pm 0.42	11.60 \pm 0.41	11.58 \pm 0.53	11.82 \pm 0.32
S-NL+Mix	33.13 \pm 0.36	31.36 \pm 0.36	32.22 \pm 0.51	12.75 \pm 0.47	13.88 \pm 0.29	15.68 \pm 0.57
S-NL+ICM	79.74\pm0.73	84.05 \pm 0.46	97.15\pm0.53	16.11 \pm 0.37	13.39 \pm 0.49	14.55 \pm 0.52
S-NL+MICM	71.07 \pm 0.37	84.15\pm0.36	96.63 \pm 0.43	16.85\pm0.48	18.90\pm0.42	16.93\pm0.51
FWD	38.48 \pm 0.34	40.01 \pm 0.53	62.91 \pm 0.38	23.36 \pm 0.27	22.44 \pm 0.54	23.77 \pm 0.42
FWD+Mix	47.35 \pm 0.38	47.98 \pm 0.43	60.35 \pm 0.56	29.63 \pm 0.36	31.75 \pm 0.45	36.85 \pm 0.52
FWD+ICM	84.13\pm0.41	90.95\pm0.45	96.72\pm0.71	37.01 \pm 0.56	43.16 \pm 0.64	62.88 \pm 0.33
FWD+MICM	80.74 \pm 0.63	87.63 \pm 0.46	95.45 \pm 0.46	38.02\pm0.42	46.17\pm0.52	63.81\pm0.45
DM	31.01 \pm 0.27	32.38 \pm 0.46	42.98 \pm 0.29	15.98 \pm 0.45	13.73 \pm 0.37	13.02 \pm 0.32
DM+Mix	26.42 \pm 0.32	33.11 \pm 0.35	37.51 \pm 0.43	14.32 \pm 0.56	14.59 \pm 0.39	13.94 \pm 0.34
DM+ICM	78.63\pm0.13	86.05\pm0.11	95.82\pm0.17	17.62 \pm 0.07	19.45 \pm 0.18	14.19 \pm 0.14
DM+MICM	73.32 \pm 0.09	80.54 \pm 0.13	90.89 \pm 0.12	19.35\pm0.07	20.86\pm0.16	17.44\pm0.10
S-EXP	37.83 \pm 0.43	40.84 \pm 0.52	44.72 \pm 0.36	11.61 \pm 0.41	11.89 \pm 0.48	14.55 \pm 0.37
S-EXP+Mix	33.59 \pm 0.43	33.12 \pm 0.34	33.85 \pm 0.38	12.17 \pm 0.31	12.71 \pm 0.41	15.82 \pm 0.36
S-EXP+ICM	73.06\pm0.06	76.24\pm0.09	79.23 \pm 0.10	15.77 \pm 0.15	14.01 \pm 0.19	17.38 \pm 0.12
S-EXP+MICM	71.28 \pm 0.08	76.18 \pm 0.11	79.27\pm0.12	16.71\pm0.09	16.30\pm0.13	20.26\pm0.16